

Full paper / Mémoire

# Photoactive sites in commercial HZSM-5 zeolite with iron impurities: An UV Raman study

Guiyang Yan, Jinlin Long, Xuxu Wang\*, Zhaohui Li, Xianzhi Fu\*

*Research Institute of Photocatalysis, Fuzhou University, Fuzhou 350002, China*

Received 11 December 2006; accepted after revision 5 March 2007

Available online 4 May 2007

## Abstract

According to our previous report [G. Yan, X. Wang, X. Fu, D. Li, *Catal. Today* 93–95 (2004) 851], commercially available HZSM-5s with different Si/Al ratio and 0.017–0.057 wt% of iron impurity have shown good photocatalytic activity for ethylene oxidation. Their activity increased with the increase of iron content. In this paper, photoactive sites in these commercial HZSM-5 zeolites were studied by UV Raman spectroscopy. The results showed that the photocatalytic activity of HZSM-5s was well correlated with the amount of two types of isolated iron species. The iron oxide and hydroxide clusters dispersed on the zeolite surface were not photocatalytically active. The possible mechanism of the photocatalysis on zeolites was also discussed. **To cite this article:** *G. Yan et al., C. R. Chimie 11 (2008).*

© 2007 Académie des sciences. Published by Elsevier Masson SAS. All rights reserved.

**Keywords:** ZSM-5; Photocatalytic activity; Iron species; UV Raman

## 1. Introduction

Recently, zeolite molecular sieves attracted considerable interest as photocatalysts. Kato et al. [1] reported that H-mordenite and H-ZSM-5s showed catalytic activity for non-oxidative coupling of methane to form C<sub>2</sub>H<sub>6</sub> under UV-light irradiation. Anpo et al. [2] found that transition-metal oxides (Ti, V, Mo, and Cr) deposited within zeolites as well as transition-metal ions (Cu<sup>+</sup>, Ag<sup>+</sup>, Pr<sup>3+</sup>) exchanged within zeolite cavities exhibited high and unique photocatalytic activities under UV irradiation for various reactions, such as the decomposition of NO<sub>x</sub> and the reduction of CO<sub>2</sub>. Sun et al.

[3] observed that toluene could be oxidized to form benzaldehyde by O<sub>2</sub> on zeolite Y under visible-light irradiation. Panov et al. [4] demonstrated that toluene and *p*-xylene could be selectively oxidized to benzaldehyde and *p*-tolualdehyde by O<sub>2</sub> on several cation-exchanged zeolites, such as NaY, BaX, and BaY, under visible-light irradiation.

Photo-excitabile materials, such as TiO<sub>2</sub>, ZnO, SrTiO<sub>3</sub>, are typical semiconductors, while zeolite molecular sieves are insulators that cannot be excited even with UV light due to a band gap of about 7 eV [5–7]. Therefore, the origin of the photocatalysis on zeolites has not been well understood. Kato et al. suggested that the highly isolated Al–O units were the photoactive sites of H-form zeolites [1]. Anpo proposed that charge-transfer pairs [Me<sup>(n-1)+</sup>–O<sup>-</sup>]\* formed upon light excitation led to the photocatalytic reactions

\* Corresponding authors.

*E-mail addresses:* [xwang@fzu.edu.cn](mailto:xwang@fzu.edu.cn) (X. Wang), [xzfu@fzu.edu.cn](mailto:xzfu@fzu.edu.cn) (X. Fu).

[2]. The photooxidations of toluene and *p*-xylene over cation-exchanged Y zeolites probably resulted from the photogenerated charged-transfer complex stabilized within zeolite channels [3,4].

We previously reported that HZSM-5 was highly active for the photocatalytic oxidation of several organic compounds [8]. It was inferred that the iron impurity contained in zeolites could be responsible for the photocatalysis. The present work aimed to find a correlation between the photocatalytic activities of HZSM-5s and different types of Fe species in the zeolites. The iron impurity of commercial HZSM-5s was well characterized by UV Raman. The results showed that the photocatalytic activity of the iron-containing zeolites depends greatly on the isolated iron–oxygen species present on the surface of the zeolites.

## 2. Experimental

### 2.1. Catalysts

HZSM-5 zeolites were prepared by an ion exchange of  $\text{NH}_4\text{NO}_3$  with NaZSM-5, followed by calcination at 500 °C. The NaZSM-5 zeolites were obtained from Nankai University, China and Zeolyst International Ltd., USA, and the HZSM-5 zeolites thus synthesized were denoted as HZSM-5-NK $x$  and HZSM-5-ZL $x$ , respectively. The number  $x$  herein stands for Si/Al ratio of the zeolites. FeZSM-5 zeolites were prepared by hydrothermal method according to the literature procedure [9], and the resultant sample was denoted as FeZSM-5-HT- $n$ . The number  $n$  stands for sample number. The resulting solid was transferred to its H-form via ion exchange with  $\text{NH}_4\text{NO}_3$ , followed by calcination at 500 °C. Si/Al ratio for the FeZSM-5-HT series samples was 36. All of the ZSM-5-based samples were MFI-type zeolites, as confirmed by X-ray diffraction analysis.

### 2.2. Photocatalytic activity

The photocatalytic oxidation of ethylene was performed at room temperature in a tubular quartz reactor (4-mm inner diameter) surrounded by four UV-light lamps (4 W, Philips) with a dominant emission at 254 nm. The UV-light lamps used in our photoreactor are placed from the catalyst at a distance of ca. 1.0 cm. The light intensity of 254 nm UV lamp of 4 W over surface of catalyst is ca.  $1.5 \text{ mW cm}^{-2}$ . The total amount of photo-over surface of catalyst is  $1.96 \times 10^{15}$ . Both the entrance and exit of the quartz reactor were connected to a 2.4-L glass container. A circulating gas pump was

set between the entrance of quartz reactor and the container. Typically, 200 mg of catalyst (30–40 mesh) was employed, and the initial concentration of ethylene in the container was about 1000 ppm, diluted with dry air. Prior to illumination, the pump was turned on till the adsorption equilibrium of ethylene was established. The concentration of ethylene and produced  $\text{CO}_2$  was monitored by a gas chromatograph (Agilent 4890 GC) equipped with a Porapak R column (80–100 mesh, 6 feet  $\times$  1/8 in.).

### 2.3. Characterization

UV Raman spectra were recorded on a self-assembled UV Raman spectrometer in the State Key Laboratory of Catalysis, Dalian Institute of Chemical Physics, Chinese Academic of Science. The UV-laser source was a Coherent Innova 300 Fred UV laser (300 cw) equipped with an intracavity frequency-doubling system using a BBO crystal to produce SHG (second harmonic generation) outputs at different wavelengths. The UV Raman spectrograph system was set up with a UV-sensitive CCD (Spex) and a triplemate (1877D, Jobin Yvon-Spex). The slit width was about 100–200  $\mu\text{m}$  and the spectral resolution was estimated to be  $4.0 \text{ cm}^{-1}$  at a slit width of 100  $\mu\text{m}$ . The power of the UV laser lines, measured from where the samples are placed, was 2.0 mW for 244.0 nm and 4.0 mW for 325.0-nm laser light.

## 3. Results and discussion

### 3.1. Chemical composition

The contents of iron and aluminum of the samples were measured by X-ray fluorescence spectroscopy (XRF, Philips PW2424F Magix) and atomic absorption spectroscopy (AAS, AA 220 type, South East Chemicals and Instruments Ltd., China), respectively, and the results are shown in Table 1. The content of iron in the HZSM-5 samples is in the range of 0.017–0.057 wt%, consistent with that reported in literature [10]. The presence of iron in a ZSM-5 type zeolite is due to the impure silicon and aluminum precursors used for zeolite synthesis, which usually contain trace amounts of iron impurities.

### 3.2. Photocatalytic activity

Fig. 1a shows that the photocatalytic activities of the HZSM-5 samples enhance with increasing iron content. No correlation between the photoactivity and the Si/Al

Table 1  
Chemical composition of HZSM-5 zeolites

Samples	Sample No.	Si/Al	XRF (wt%)		AAS (wt%)	
			Al	Fe	Al	Fe
Commercially available HZSM-5	HZSM-5-NK25	25	2.3	0.043		
	HZSM-5-NK38	38	1.7	0.050		
	HZSM-5-NK50	50	1.2	0.057		
	HZSM-5-ZL60	60	2.2	0.022		
	HZSM-5-ZL100	100	1.1	0.024		
	HZSM-5-ZL160	160	0.7	0.017		
Hydrothermally synthesized FeZSM-5	FeZSM-5-HT-1	36	1.3	0.82		
	FeZSM-5-HT-2	36	1.2	0.37		
	FeZSM-5-HT-3	36	1.5	0.21		
	FeZSM-5-HT-4	36	1.2	0.15		
	FeZSM-5-HT-5	36	1.1	0.060		

ratios or the content of Al can be found. This indicates that the iron species are photoactive species, and that the aluminum species is inactive for the oxidation of ethylene. In order to investigate the role of iron species further, we specially synthesized FeZSM-5 zeolites and tested their photocatalytic activities. Beyond our expectation, the photocatalytic activity of the FeZSM-5 zeolite series does not increase when the Fe content enhances. Over the FeZSM-5-HT-*n*, the conversion of ethylene decreases from 38% to 5% when the iron amount increases from 0.06 to 0.82 wt% (Fig. 1b), and even FeZSM-5-HT-5 shows less photocatalytic efficiency than HZSM-5-NK50, although they have nearly the same content of iron. The difference in the activities between the FeZSM-5-HT-5 and the commercial HZSM-5-NK50 can result in the different contents of

the active iron species. In fact, the chemical states of iron in a Fe-containing ZSM-5 zeolite are very complicated according to the literature. The iron species introduced by different methods have a significant effect on the photocatalytic performance of the zeolites due to the different chemical nature of the iron species introduced by different methods. It is therefore desirable to study the chemical nature, particularly the local structure, of the iron species in the photocatalytically active zeolites.

### 3.3. UV Raman spectroscopy

The UV Raman spectra were measured on all the commercial HZSM-5 (NK $x$  and ZL $x$ ) under the excitation of 244-nm laser light. The experiments were based on the  $O^{2-}-Fe^{3+} \rightarrow O^{-}-Fe^{2+}$  ligand-to-metal charge-transfer transition (LMCT) in resonant Raman conditions. In fact, for tetrahedrally coordinated  $Fe^{3+}$  this LMCT exhibits an absorption band centered around 220 nm [11,12]; see also Ref. [8]. All samples exhibit similar UV Raman spectra (Fig. 2), peaking at 296, 380 (very strong), 465 (shoulder), 802, 1000–1280 (strong and broad), 1556, and 2332  $cm^{-1}$ . According to literature [11], the bands at 380 and 802  $cm^{-1}$  are assigned to the five-membered building unit of the MFI-structured zeolite and the framework symmetric stretching vibration of ZSM-5s, respectively. The broad band in the region from 1000 to 1280  $cm^{-1}$  is inconsistent with that of the FeZSM-5 referenced in the literature [11]. The broad band could be divided into three peaks centered at 1092, 1173, and 1228  $cm^{-1}$  using a Gaussian fit analysis (Fig. 2-inset). These three peaks at 1092, 1173 and 1228  $cm^{-1}$  significantly shift by 50–60  $cm^{-1}$  to a longer wavenumber compared to those reported in the literature (1022, 1125 and 1175  $cm^{-1}$ ). The reason for this shift is not well understood, probably

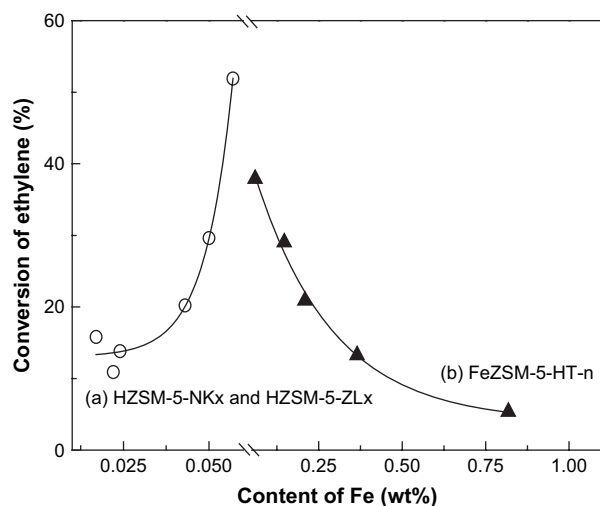


Fig. 1. Photocatalytic activity of HZSM-5 and FeZSM-5 zeolites as a function of Fe content.

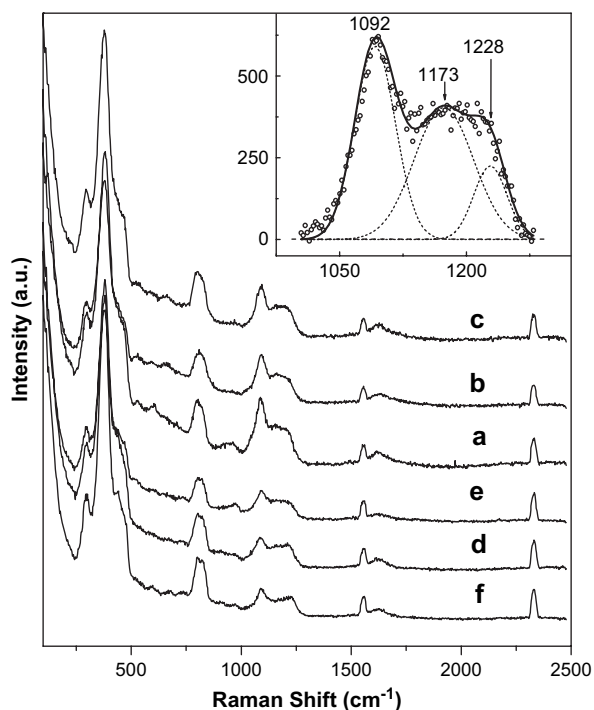


Fig. 2. UV Raman spectra ( $\lambda_{\text{ex}} = 244 \text{ nm}$ ) of the HZSM-5 samples. (a) NK25, (b) NK38, (b) NK50, (d) ZL60, (e) ZL100, (f) ZL160. The inset is deconvoluted sub-bands of UV Raman spectra in the region of  $1000\text{--}1280 \text{ cm}^{-1}$  of NK50. Experiment (hollow dots), Gaussian fitting (solid line), sub-bands (dashed line).

resulting from the difference in the local structure of iron species between different series of ZSM-5 samples. However, by far, the assignment to the broad band in the region from  $1000$  to  $1280 \text{ cm}^{-1}$  has not been unambiguous. Li et al. suggested that these bands should be assigned to the asymmetric vibrations of the isolated Fe–O–Si species [11]. Interestingly, two symmetric vibrational modes at  $516$  and  $580 \text{ cm}^{-1}$ , corresponding to the isolated Fe–O–Si species in FeZSM-5, do not appear for all of the samples. In the region  $1000\text{--}1250 \text{ cm}^{-1}$ , the  $\nu_{\text{asym}}(\text{Si-O-Si})$  modes are Raman inactive [12]. When heteroatoms M were inserted in the MFI framework, in the case of  $\text{Ti}^{4+}$  a strong band at  $1125 \text{ cm}^{-1}$ , corresponding to the totally symmetric stretching mode of the  $[\text{Ti}(\text{O-Si})_4]$  units, was observed clearly [13,14]. As far as our samples are concerned, the three bands in the region  $1000\text{--}1280 \text{ cm}^{-1}$  should be attributed to the totally symmetric stretching mode of the  $[\text{Fe}(\text{O-Si})_4]$  units because of the incorporation of the trace amount of iron impurities into the ZSM-5 zeolite framework during hydrothermal synthesis.

Raman scattering can come from the surface and from the bulk of the solid, but the signal from the

bulk is attenuated when the sample strongly absorbs the excitation laser light as well as the scattering light [15]. Since iron species absorbs the UV laser light strongly, UV Raman spectra observed in our samples should mostly result from iron species on the zeolite surface. Based on the fact that the relative area of the broad Raman band at  $1000\text{--}1280 \text{ cm}^{-1}$  (to the band at  $380 \text{ cm}^{-1}$  as an internal standard [10]) increases almost linearly with the total content of iron in the samples (Fig. 3), it is deduced that all iron atoms can be on the top of the zeolite framework. Moreover, it is interesting to note that the total area of the bands at  $1092$  and  $1173 \text{ cm}^{-1}$  (relative to that at  $380 \text{ cm}^{-1}$ ) increases almost linearly with the yield of ethylene conversion (Fig. 4), whereas the band area at  $1228 \text{ cm}^{-1}$  shows an uncertain trend. This correlation suggests that some particular iron species, which exists on the surface, exhibits Raman signals at  $1092$  and  $1173 \text{ cm}^{-1}$ , and may be responsible for the observed photocatalytic activity on the commercial HZSM-5.

When  $325\text{-nm}$  laser light was used as the excitation source, no useful Raman signals can be observed for all the samples except the vibration bands of the zeolite at  $380$  and  $802 \text{ cm}^{-1}$  (Fig. 5). In fact, the ethylene conversion over the zeolites is much less under  $365\text{-nm}$  irradiation than under  $254\text{-nm}$  irradiation. This constitutes the additional evidence that the zeolite only shows photocatalytic activity when the iron species are effectively excited by low-wavelength UV light.

According to the above results, the photocatalytic activity of HZSM-5 is related to two types in three isolated iron species. Unfortunately, such characterization which we have carried out could not distinguish among

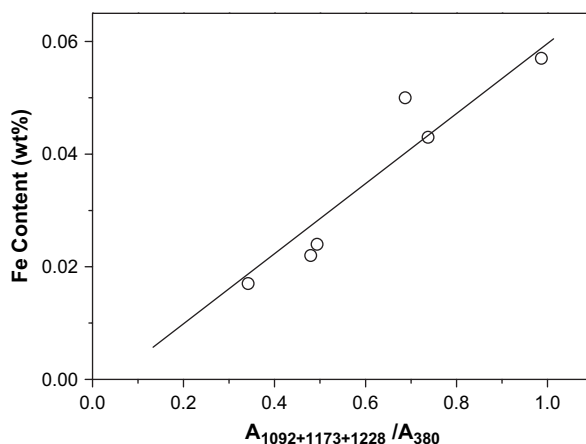


Fig. 3. Fe content of the HZSM-5 samples versus the ratio of the total area of the three UV Raman bands at  $1000\text{--}1280 \text{ cm}^{-1}$  ( $A_{1092+1173+1228}$ ) to the area of the band at  $380 \text{ cm}^{-1}$  ( $A_{380}$ ).

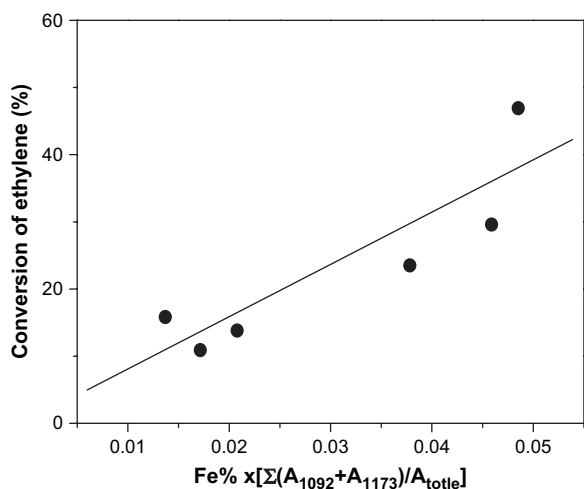


Fig. 4. Photocatalytic conversion of ethylene versus the Fe content of the UV Raman bands at 1092 and 1173  $\text{cm}^{-1}$  ( $A_{1092+1173}$ ) of the HZSM-5 samples.

the three types of Fe species. But it is not difficult to understand the photocatalytic activity order among the three NK $x$  samples (NK50 > NK38 > NK25) based on the above analysis.

Photoinduced reaction of organic compounds on a semiconductor, such as  $\text{TiO}_2$ , is considered to be initiated by the valence band hole and conduction band electron formed by UV light excitation. For the ZSM-5, when the iron species are isolated in tetrahedral oxygen environment of the zeolite framework, the Fe–O of isolated  $[\text{FeO}_4]$  units may be excited to form an excitation state  $[\text{Fe}^{2+}-\text{O}^-]^*$  under 254-nm light irradiation

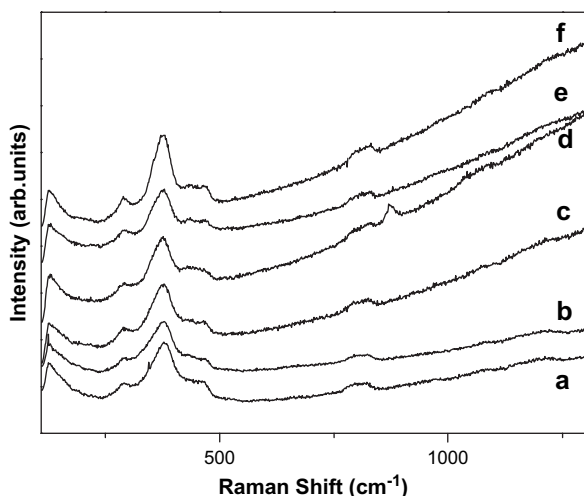


Fig. 5. UV Raman spectra ( $\lambda_{\text{ex}} = 325 \text{ nm}$ ) of the commercial HZSM-5 samples. (a) NK25, (b) NK38, (c) NK50, (d) ZL60, (e) ZL100, (f) ZL160.

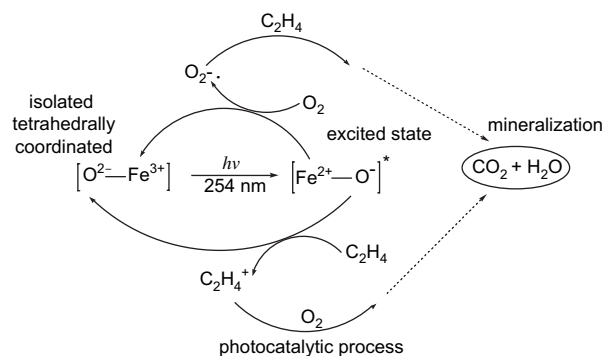


Fig. 6. Suggested mechanism for photocatalytic oxidation of ethylene on HZSM-5.

as shown by UV Raman (Figs. 2 and 5) and DRS spectra [8]. The  $[\text{Fe}^{2+}-\text{O}^-]^*$  may activate both  $\text{O}_2$  and ethylene molecules, leading to the oxidation of ethylene to  $\text{CO}_2$  and  $\text{H}_2\text{O}$  by  $\text{O}_2$  (Fig. 6). This mechanism, based on the suggestion by Anpo et al. [2], could be well applied in the understanding of the photocatalytic behavior on metal-containing zeolites.

#### 4. Conclusions

With only ca. 0.02–0.06 wt% of iron impurities, the commercially available HZSM-5 is highly photocatalytically active for the oxidation of ethylene under 254-nm UV irradiation and the activity increases with increasing iron content, whereas the hydrothermally synthesized FeZSM-5 showed a decreasing activity with increasing Fe content. By means of UV Raman spectroscopy, a well-defined linear relationship between the photocatalytic activity and the bands at 1092 and 1173  $\text{cm}^{-1}$  (relative to that at 380  $\text{cm}^{-1}$ ) is established. It was revealed that two types of the isolated iron species in the zeolite framework are responsible for the photocatalytic activity. The iron oxide and hydroxide clusters dispersed in the pore surface of the zeolite are not photocatalytically active.

#### Acknowledgments

This work was supported by the National Foundation of Natural Science of China (Nos. 20673020, 20573020, 20373011, 20537010, 20677010), and the National Key Basic Research Special Foundation (2004CCA07100). The authors thank Professor Can Li, State Key Laboratory of Catalysis in Dalian Institute of Chemical Physics, Chinese Academy of Science for UV Raman spectroscopy determinations.

**References**

- [1] Y. Kato, H. Yoshida, A. Satsuma, T. Hattori, *Microporous Mesoporous Mater.* 51 (2002) 223.
- [2] M. Anpo, M. Matsuoka, Y. Shioya, H. Yamashita, *J. Phys. Chem.* 98 (1994) 5744.
- [3] H. Sun, F. Blatter, H. Frei, *J. Am. Chem. Soc.* 116 (1994) 7951.
- [4] A.G. Panov, R.G. Larsen, N.I. Totah, S.C. Larsen, V.H. Grassian, *J. Phys. Chem. B* 104 (2000) 5706.
- [5] N. Zheng, X. Bu, B. Wang, P. Feng, *Science* 298 (2002) 2366.
- [6] A.E.C. Palmqvist, B.B. Iversen, E. Zanghellini, M. Behm, G.D. Stucky, *Angew. Chem., Int. Ed.* 43 (2004) 700.
- [7] G. Calzaferri, C. Leiggenger, S. Glaus, D. Schürch, K. Kuge, *Chem. Soc. Rev.* 32 (2003) 29.
- [8] G. Yan, X. Wang, X. Fu, D. Li, *Catal. Today* 93–95 (2004) 851.
- [9] R.J. Argauer, Md. Kensington, G.R. Landolt, N.J. Audubon, U.S. Patent 3,702,886, 1972.
- [10] L.V. Pirutko, V.S. Chernyavsky, A.K. Uriarte, G.I. Panov, *Appl. Catal. A: General* 227 (2002) 143.
- [11] C. Li, *J. Catal.* 216 (2003) 203.
- [12] S. Bordiga, A. Damin, F. Bonino, G. Ricchiardi, A. Zecchina, R. Tagliapietra, C. Lamberti, *Phys. Chem. Chem. Phys.* 54 (2003) 390.
- [13] G. Ricchiardi, A. Damin, S. Bordiga, C. Lamberti, G. Spanò, F. Rivetti, A. Zecchina, *J. Am. Chem. Soc.* 123 (2001) 11409.
- [14] C. Li, G. Xiong, Q. Xin, J. Liu, P. Ying, Z. Feng, J. Li, W. Yang, Y. Wang, G. Wang, X. Liu, M. Lin, X. Wang, E. Min, *Angew. Chem., Int. Ed.* 38 (1999) 2220.
- [15] M. Li, Z. Feng, G. Xiong, P. Ying, Q. Xin, C. Li, *J. Phys. Chem. B* 105 (2001) 8107.